Trend analysis from 1970 to 2008 and model evaluation of EDGARv4 global gridded anthropogenic mercury emissions*

Marilena Muntean, Greet Janssens-Maenhout, Shaojie Song, Noelle E. Selin, Jos G.J. Olivier, Diego Guizzardi, Rob Maas and Frank Dentener

MIT JOINT PROGRAM ON THE SCIENCE AND POLICY of GLOBAL CHANGE

*Reprinted from
Science of the Total Environment, 494-495(2014): 337-350

Reprint 2014-15

The MIT Joint Program on the Science and Policy of Global Change combines cutting-edge scientific research with independent policy analysis to provide a solid foundation for the public and private decisions needed to mitigate and adapt to unavoidable global environmental changes. Being data-driven, the Program uses extensive Earth system and economic data and models to produce quantitative analysis and predictions of the risks of climate change and the challenges of limiting human influence on the environment—essential knowledge for the international dialogue toward a global response to climate change.

To this end, the Program brings together an interdisciplinary group from two established MIT research centers: the Center for Global Change Science (CGCS) and the Center for Energy and Environmental Policy Research (CEEPR). These two centers—along with collaborators from the Marine Biology Laboratory (MBL) at Woods Hole and short- and long-term visitors—provide the united vision needed to solve global challenges.

At the heart of much of the Program's work lies MIT's Integrated Global System Model. Through this integrated model, the Program seeks to: discover new interactions among natural and human climate system components; objectively assess uncertainty in economic and climate projections; critically and quantitatively analyze environmental management and policy proposals; understand complex connections among the many forces that will shape our future; and improve methods to model, monitor and verify greenhouse gas emissions and climatic impacts.

This reprint is one of a series intended to communicate research results and improve public understanding of global environment and energy challenges, thereby contributing to informed debate about climate change and the economic and social implications of policy alternatives.

Ronald G. Prinn and John M. Reilly,
Program Co-Directors

For more information, contact the Program office:
MIT Joint Program on the Science and Policy of Global Change

Postal Address:
Massachusetts Institute of Technology
77 Massachusetts Avenue, E19-411
Cambridge, MA 02139 (USA)

Location:
Building E19, Room 411
400 Main Street, Cambridge

Access:
Tel: (617) 253-7492
Fax: (617) 253-9845
Email: ***globalchange@mit.edu***
Website: ***http://globalchange.mit.edu/***

Science of the Total Environment 494–495 (2014) 337–350

Contents lists available at ScienceDirect

Science of the Total Environment

journal homepage: www.elsevier.com/locate/scitotenv

Trend analysis from 1970 to 2008 and model evaluation of EDGARv4 global gridded anthropogenic mercury emissions

Marilena Muntean [a,*], Greet Janssens-Maenhout [a], Shaojie Song [b], Noelle E. Selin [b], Jos G.J. Olivier [c], Diego Guizzardi [a], Rob Maas [d], Frank Dentener [a]

[a] European Commission, Joint Research Centre, Institute for Environment and Sustainability, Ispra, Italy
[b] Massachusetts Institute of Technology, Cambridge, MA, United States
[c] PBL Netherlands Environment Assessment Agency, Bilthoven, the Netherlands
[d] RIVM National Institute for Public Health and Environment, Bilthoven, the Netherlands

HIGHLIGHTS

- A global mercury emission inventory over the past four decades was established.
- The inventory was at the lower range of the UNEP Minamata estimates.
- The inventory was evaluated using a global 3-D mercury model GEOS-Chem.
- The model reproduced spatial variations and long-term trends.

ARTICLE INFO

Article history:
Received 26 February 2014
Received in revised form 3 June 2014
Accepted 4 June 2014
Available online xxxx

Editor: Mae Sexauer Gustin

Keywords:
Mercury emissions
Global gridmaps
End-of-pipe impacts
Inventory evaluation
Atmospheric modelling
Artisanal and small-scale gold production

ABSTRACT

The Emission Database for Global Atmospheric Research (EDGAR) provides a time-series of man-made emissions of greenhouse gases and short-lived atmospheric pollutants from 1970 to 2008. Mercury is included in EDGARv4.tox1, thereby enriching the spectrum of multi-pollutant sources in the database. With an average annual growth rate of 1.3% since 1970, EDGARv4 estimates that the global mercury emissions reached 1287 tonnes in 2008. Specifically, gaseous elemental mercury (GEM) (Hg^0) accounted for 72% of the global total emissions, while gaseous oxidised mercury (GOM) (Hg^{2+}) and particle bound mercury (PBM) (Hg-P) accounted for only 22% and 6%, respectively. The less reactive form, i.e., Hg^0, has a long atmospheric residence time and can be transported long distances from the emission sources. The artisanal and small-scale gold production, accounted for approximately half of the global Hg^0 emissions in 2008 followed by combustion (29%), cement production (12%) and other metal industry (10%). Given the local-scale impacts of mercury, special attention was given to the spatial distribution showing the emission hot-spots on gridded 0.1° × 0.1° resolution maps using detailed proxy data. The comprehensive ex-post analysis of the mitigation of mercury emissions by end-of-pipe abatement measures in the power generation sector and technology changes in the chlor-alkali industry over four decades indicates reductions of 46% and 93%, respectively. Combined, the improved technologies and mitigation measures in these sectors accounted for 401.7 tonnes of avoided mercury emissions in 2008. A comparison shows that EDGARv4 anthropogenic emissions are nearly equivalent to the lower estimates of the United Nations Environment Programme (UNEP)'s mercury emissions inventory for 2005 for most sectors. An evaluation of the EDGARv4 global mercury emission inventory, including mercury speciation, was performed using the GEOS-Chem global 3-D mercury model. The model can generally reproduce both spatial variations and long-term trends in total gaseous mercury concentrations and wet deposition fluxes.

1. Introduction

Mercury emitted from both natural and anthropogenic sources is transported long distances in the atmosphere and, ultimately, affects ecosystems and human health (Karagas et al., 2012; Mahaffey et al., 2011; Mergler et al., 2007). United Nations Environment Programme

* Corresponding author at: European Commission, Joint Research Centre, Institute for Environment and Sustainability, Ispra (VA), 21027, Via E. Fermi 2749, Italy. Tel.: +390332785539.
E-mail addresses: marilena.muntean@jrc.ec.europa.eu, marilena.muntean@gmail.com (M. Muntean).

http://dx.doi.org/10.1016/j.scitotenv.2014.06.014

(UNEP) (2013a) concluded that current anthropogenic emissions contribute approximately 30% of the total annual emissions into the atmosphere; geological sources account for an additional 10%, while legacy "re-emissions" of mercury accumulated over the last several decades in soils and oceans account for 60%. The recently adopted Minamata Convention (UNEP, 2013b) addresses anthropogenic emissions, agrees to ban the trade of various mercury-containing products by 2020, and mandates controls on mercury in specific sectors.

Based on our current knowledge on anthropogenic mercury species behaviour in the atmosphere, elemental mercury (Hg^0) can be transported over long distances, while gaseous oxidised mercury (Hg^{2+}) and particle bound mercury (Hg-P), which are the reactive forms of mercury, have shorter lifetimes and are deposited close to their emission sources (Steffen et al., 2008). Therefore, an important component of evaluating the emission strength and the resulting local-scale effects of different mercury species is the resolution of gridded emissions combined with the quality of proxy data used for determining emission distributions.

Relationships between human activities, changes in atmospheric concentrations and removal by deposition are described by atmospheric transport and chemistry modelling coupled with parameterisations for ocean and terrestrial ecosystem re-emissions. Comprehensive results on the discrepancy between measured and modelled oxidised mercury species highlight the need for better mercury species emission inventories (Zhang et al., 2012a) and better techniques to measure the oxidised species (Gustin et al., 2013; Kos et al., 2013; Steffen et al., 2008; Swartzendruber et al., 2008). Moreover, recent analyses of mercury chemistry uncertainties in atmospheric modelling (Subir et al., 2011, 2012) also underline the lack of a proper understanding of the chemical reaction mechanisms for many mercury reactions. Model improvement requires reliable monitoring data for different mercury forms (Ryaboshapko et al., 2007), which should include both hemispheres and various media (HTAP, 2010; UNEP, 2013a). Moreover, the complexity of mercury interactions increases when considering the continuous exchange via mercury fluxes between terrestrial, aquatic and atmosphere earth components (ACAP, 2005; Amos et al., 2013; Selin, 2009) as part of the global mercury cycle. For example, it has been suggested that multi-media modelling (Travnikov and Ilyin, 2009) is imperative to understand transfer of mercury across land–air–water and ice interfaces, e.g. to explain mercury deposition in the Arctic (AMAP, 2011).

Anthropogenic mercury emissions, which vary temporally depending on the effects of emerging economies and the mitigation policies implemented in different regions, originate from primary contributing sectors, e.g., non-ferrous metal production, iron and steel production, the chlor-alkali industry, cement production, waste incineration and combustion in power generation and residential and industrial activities. In this study, we extend the EDGARv4 database with information relevant for mercury emissions that encompasses all of the important sources. Moreover, we assess the effectiveness of previously implemented mitigation policies. For artisanal and small-scale gold production, which is an important sector with limited available information and is characterised by large uncertainty, this work proposes a sector-specific approach that is based on gold market demand as the driver of the mercury emission time series over the period 1970–2008. Removal efficiencies of the existing emission control device systems for SO_x, NO_x and particulate matter (PM) are also important elements for assessing anthropogenic Hg emission reductions. Their capability to mitigate mercury emissions has been demonstrated in previous studies. Recent studies present quantitative results (Park et al., 2008; Pudasainee et al., 2010, 2012; Srivastava et al., 2003) and document the complex factors that lead to mercury speciation, which strongly depends on the emission control system configuration, fuel characteristics and combustion parameters; nevertheless, further investigations are needed to reach a satisfactory level of agreement on the chemical behaviour of mercury species for different control systems. Here, we make use of the EDGARv4 capability to distinguish between control devices and their combinations for each power plant type described in the international specialised datasets to perform a comprehensive ex-post analysis (backwards looking) of the effects of mitigation policies that have been implemented in different world regions over 1970–2008.

Previous global anthropogenic mercury inventories (Pacyna et al., 2006, 2010; Pirrone et al., 2010; Rafaj et al., 2013; Streets et al., 2011) exhibit variability in global emission totals, which is illustrated in Table S1 of the Supplementary Information (SI), due to the use of different key sectors with different aggregated subsector compositions and the approaches used to derive activity data, emission factors and reduction percentages. Regarding emission trends, Streets et al. (2011) applied a consistent methodology to estimate mercury emissions beginning in 1850, whereas UNEP (Pacyna et al., 2006, 2010; UNEP, 2010) focused on improving each subsequent version; therefore, a year-to-year comparison is not possible because of the methodological differences.

The EDGARv4 mercury inventory, which is primarily based on activity data from international statistics and emission factors from official datasets, is designed to provide high-resolution independent estimates that are consistent across all world countries over four decades and includes detailed technology specifications that allow us to assess the effectiveness of the mitigation measures implemented so far and their future potential. Special attention is given to sectors exhibiting the largest uncertainties by developing new approaches to derive emission factors for the chlor-alkali industry and activity data for artisanal and small-scale gold production compared to other prior assessments. Therefore, the effectiveness of emission reduction measures in certain areas combined with a clear understanding of changes in recent mercury emission patterns could foster further decisions on mercury mitigation in different regions. Moreover, we evaluate the EDGARv4 gridded anthropogenic emission inventory using the GEOS-Chem global 3-D mercury model, which is a "state-of-the-art" chemical transport model, and available observational data of TGM (total gaseous mercury, Hg^0 and Hg^{2+}) concentrations and wet deposition fluxes assembled from several monitoring networks and individual sites. EDGARv4 aims for global coverage with an emphasis on consistency and comparability that encompasses the various regions, sectors and pollutants. However, the trade-off is that the emission inventory is unable to contain regional details and remains less accurate at the national level, which is illustrated in Table S2 of the SI for China's zinc smelters (Wu et al., 2012) and cement production in Korea (Won and Lee, 2012).

The purpose of this study was to explore if large scale features and temporal trends of mercury atmospheric observations could be reproduced using a global gridded mercury emission inventory over 4 decades as input for a chemical transport model. This paper describes EDGARv4.tox1 (hereafter called EDGARv4) and its application in a 3-D model with the following structure. Section 2 describes the EDGARv4 technology-based methodology, providing details on activity data, emission factors, mercury removal efficiencies for existing control devices, the approach used to distribute emissions on gridmaps and a description of the modelling tool used to evaluate the emission inventory at a global scale. Section 3 presents the results and includes historical global trend and ex-post mercury mitigation analysis and describes the EDGARv4 gridded mercury emissions as input for chemical transport models; the results of the inventory evaluation from the GEOS-Chem global mercury simulation are also discussed in Section 3. This section also includes a description on global mercury emission time series for EDGARv4 with a detailed breakdown for each sector and country/region, which is compared to the widely used UNEP mercury emission inventory for 2005 (UNEP, 2010). The main findings are discussed in Section 4; conclusions are presented in Section 5.

Further updates and use of this emission inventory are envisaged in a chain that connects the emission inventory with concentration measurements and health impacts via chemical transport modelling. Moreover, the multi-pollutant benefits of sector-specific emission reductions, which utilises air pollutants and greenhouse gases (GHGs) in EDGARv4, enable country-specific choices regarding mitigation measures to reduce multi-pollutants in different sectors.

2. Methodology

2.1. EDGAR technology-based methodology applied to mercury emissions

Generally, emissions are calculated using the equation

$$EM = AD * EF, \quad (1)$$

where EM is the pollutant emission, AD corresponds to the activity data and EF represents the emission factor. The technology-based methodology that is used in our approach considers information regarding technologies and control measures where available. The total country-wide annual emission of total mercury (Hg) in EDGARv4 is determined using

$$EM_C(t, x_l) = \sum_{i,j,k}[AD_{C,i}(t) * TECH_{C,i,j}(t) * EOP_{C,i,j,k}(t) * EF_{C,i,j}(t, x_l) * \left(1 - RED_{C,i,j,k}(t, x_l)\right) * f_{C,i,j}(x_l)] \quad (2)$$

where indices C, i, j, and k indicate that the term is country-specific, sector-specific, technology-specific and control measure-specific; AD corresponds to technology-based activity data, which represents activity data allocated to a certain technology (TECH) and control measure (EOP), the TECH and EOP are included as %; EF is the technology-based emission factor, which is the emission factor of a specific activity associated with a certain technology; RED represents the control measure included as % reduction of the uncontrolled EF; f is the speciation factor; EM is the emission for a country C in function of time and substance x, species l.

Three different mercury species are distinguished in this study. For each species, the emission factors are estimated with a simplified approach using $EF_{C,i,j}(Hg_{Spec}) = f_i * EF_{C,i,j}(Hg)$ for each sector, where $EF_{C,i,j}(Hg)$ is the emission factor for the total mercury for sector i and technology j, f_i is the speciation split factor (%) for sector i, and $EF_{C,i,j}(Hg_{Spec})$ is either the emission factor for gaseous Hg^0, Hg^{2+}, or particle bound Hg-P.

For each country, the mercury emissions are spatially distributed using proxy data, e.g., point source locations, and urban and rural population data where detailed information on source locations is not available.

A schematic of the EDGAR approach is presented in Fig. S1 of the SI.

2.1.1. Activity data, technology and control measures

Human activities represented in this study include the metal and chlor-alkali industries, cement production, waste incineration, and combustion in power generation, manufacturing industries and residential activities, which correspond to the important mercury emitting sectors.

EDGARv4 contains activity data that are primarily derived from international statistics. Fuel production and combustion statistics obtained from the International Energy Agency (IEA, 2009) database are used to calculate energy-related emissions, which include combustion in the energy, manufacturing and transformation industries, combustion in oil refineries and the residential sector. Data for the production of iron and steel, non-ferrous metals, and non-metallic minerals in EDGARv4 were obtained from the U.S. Geographical Survey (USGS) (2011) and UN commodity statistics (UN) (2011); and information from the Food and Agricultural Organization (FAO) (2011) was used for agricultural waste burning. The amounts of each waste type (i.e., municipal, hospital and industrial) in the waste incineration sector were collected from country submissions to the UNFCCC considering the shares of incineration and landfilling for the years 1990 and 2005. The activity data were retrofitted for years between 1970 and 1990, and we assumed that the ratio of landfilling and incineration without energy recovery remained constant for this period. For Non-Annex I countries, only municipal waste incineration was included, using the shares of incineration and landfilling reported by IPCC (2006) and the landfilled amount as the basis for the activity data. For the full derivation of the waste activity data is referred to Olivier and Janssens-Maenhout (2012).

Activity data for artisanal and small-scale gold production and chlorine production using mercury cell technology in the chlor-alkali industry were estimated using information from specialised organisations and from the scientific literature; details on these estimates are provided below. Artisanal and small-scale gold production includes gold mining in which rudimentary practices are still used, such as whole-ore mercury amalgamation, open burning without mercury capture, and the use of cyanide with mercury or after mercury use (UNEP, 2012), which release a large amount of mercury into the environment. This activity, which is illegal in most countries, is consequently not included in official reports. Moreover, mercury emission factors resulting from amalgamation processes are not well known; this lack of information leads to a large uncertainty in emission estimations. In this work, the mercury consumption data for artisanal and small-scale gold production estimated by Telmer and Veiga (2008) were used as EDGARv4 activity data in 2008. Our approach to construct activity data back to 1970 is based on the gold market demand as a driver and consists of applying the trends in large-scale gold production to recent information on mercury consumption in artisanal and small-scale gold production for each country from Telmer and Veiga (2008). The global trend in large-scale gold production was used to estimate the activity data time series for countries with no reported industrial-scale gold production. With this approach a consistent activity dataset was derived for this sector from 1970 to 2007 based on reliable USGS large-scale gold production data. The resulting global trend in mercury used in artisanal and small-scale gold production from 1970 to 2007 (2008) is illustrated in Fig. S2 of the SI. In 2008, the highest mercury consumptions in the artisanal and small-scale gold production sector occurred in China (45%), Indonesia (15%) and Columbia (8%).

The chlor-alkali process uses electrolysis of sodium chloride to produce chlorine, caustic soda and other products. Three main technologies rely on mercury cells, diaphragm cells, and membrane cells. Because only mercury cell technology emits mercury, the global mercury emission trend from this sector is related mainly to the progressive conversion from mercury cell technology to diaphragm and membrane cell technologies. Therefore, information on chlorine or caustic soda production (with a conversion factor of 1/1.1; Eurochlor (1998)) using this specific technology was collected from the UN commodity statistics, Eurochlor, World Chlorine Council and Zero Mercury Working Group studies; gaps in the obtained data were filled using country reports and the scientific literature (ABICLOR, 2004, 2005, 2006, 2007, 2008, 2010; Ayers, 1997; JSIA, 2011; Mukherjee et al., 2009; Sznopek and Goonan, 2000). When mercury cell chlorine capacity data were available, an average operating capacity of 90% (Mahan and Saviz, 2007) was considered for deriving chlorine production activity data.

In EDGARv4, technologies are represented for iron and steel production, and combustion in power generation and from residential activities; in addition, NO_x, PM, SO_x and combined control measures (IEA, 2005; Platts, 2006) are associated with technologies in the power generation sector for power plants in each country (which are listed in Table S3 of the SI).

2.1.2. Emission factors and speciation

The emission factors (EFs) used to calculate mercury emissions for the energy sector are primarily from official emission factor datasets (EMEP/EEA, 2009; US_EPA/AP42, 2011) (Table S4 of the SI). The US

EPA/AP42 (2011) uncontrolled mercury emission factors were used for lignite, bituminous, and sub-bituminous coal with dry bottom boiler technology; these factors are consistent with the findings of Wang et al. (2010) for China.

Because not all mercury-emitting activities in non-ferrous metal production are included in the EMEP/EEA air pollutant emission inventory guidebook, the emission factors for large-scale gold production and mercury production were obtained from Pacyna et al. (2010), while the emission factor for artisanal and small-scale gold mining activity is based on information presented by Telmer and Veiga (2008). Table S5 of the SI indicates the ranges of EFs for the production of chemicals (mercury cell technology in the chlor-alkali industry), iron and steel, non-ferrous metals, non-metallic minerals (cement). Special attention is given to the estimation of EFs for cement in relation to clinker, waste incineration, and chlorine produced with mercury cell technology; this estimation is described further below.

Mercury emissions from cement production are highly dependent on the clinker-to-cement ratio. Recent studies have shown that from 1990 to 2005, the clinker-to-cement ratio decreased from approximately 0.81 to 0.77 (Moya et al., 2010; WBCSD, 2009), which could indicate a recent decrease in emission factors for different countries and/or regions. Therefore, a country-specific approach that is based on the percentage of clinker in cement is needed. In this study, emission factors were derived by considering the emission factor expressed per mass of clinker produced (EMEP/EEA, 2009) and the in-house EDGAR dataset of clinker content in cement for each country from 1970 to 2008. The variation of clinker content in cement (%), which was used to calculate mercury emissions from cement production, for different regions of the globe is illustrated in Fig. S3 of the SI.

Mercury emission factors for solid waste incineration were obtained from EMEP/EEA (2009). Specific controlled and uncontrolled EFs were assigned to municipal, hospital, and industrial waste types for industrialised and developing country groups. In addition, information on mitigation measures from Takahashi et al. (2010) were used to estimate the mercury EFs for municipal solid waste incineration in Japan. The EFs used in this work to estimate mercury emissions from municipal solid waste incineration are provided in Fig. S4 of the SI.

In the chlor-alkali industry, especially for mercury cell technology, various mitigation measures (e.g., best available techniques, which include integrated process measures that are related to mercury recovery and leakage limitation) have been recently implemented in some regions, which has reduced the mercury emissions per ktonne of chlorine produced; the EF trends used in this study for Europe, industrialised countries and the rest of the world are presented in Fig. S5 of the SI. This approach consists of a complete EF dataset formed using EFs for Europe with information from Eurochlor and assuming that the mitigation measures in other regions have been implemented later and primarily after 2000. Other industrialised countries reached the same level as Europe in 2008, while the remainder of the world attained the EMEP/EEA (2009) uncontrolled emission factor level of approximately 4.8 kg/ktonne in 2008. However, according to the country-specific emission factors, e.g., the emission factor used in India to calculate mercury emissions in the chlor-alkali industry for the period 2000–2004 is approximately 20.4 g/tonne caustic soda (Mukherjee et al., 2009), the uncertainty in emission estimation for this activity remains large.

Emission factors for mercury species (gaseous elemental mercury (Hg^0), gaseous oxidised mercury (Hg^{2+}) and particle bound mercury (Hg-P)) are also included in EDGARv4. EFs were calculated by multiplying the total mercury emission factors by the speciation split factors recommended by AMAP/UNEP (2008) (described in Table S6 of the SI).

2.1.3. Mercury removal efficiency of existing control devices in the power generation sector

Large amounts of mercury can be removed in power generation using existing air pollution control devices. Based on the data and information from the Platts-World Electric Power Plants database (Platts, 2006) and the IEA Clean Coal Centre CoalPower5 database (IEA, 2005), the following technology and country-specific shares of existing control systems were assigned to the power plant sector in EDGARv4: electrostatic precipitator (ESP), fabric filter (FF), SO_2 scrubbers (dry FGD and wet FGD) and selective catalytic reduction (SCR). However, the implementation of mercury regulatory requirements in some countries could lead to a higher percentage of mercury reduction by retrofitting existing control devices (Foerter and Whiteman, 2005).

The complex chemical behaviour of mercury and its species in flue gas for different control devices makes it difficult to allocate removal efficiencies to individual or combined mitigation systems. Wang et al. (2010) showed that ESPs do not remove reactive gaseous mercury (Hg^{2+}); however, some gaseous elemental mercury (Hg^0) can be absorbed or oxidised into Hg^{2+} or Hg-P when cooled to 400 °C; the latter is largely removed by ESP, leading to a large decrease in the concentration of Hg. SCR oxidises some Hg^0 to Hg^{2+}, which is water soluble and can be removed in flue gas desulphurisation (FGD) systems. However, Hg^0 is water insoluble; therefore, Hg^0 is difficult to remove. Another study (Tang et al., 2007) indicates that most Hg-P and Hg^{2+} are removed using wet FGD. Mercury capture in mitigation devices is highly dependent on the coal characteristics, flue gas composition, fly ash properties and flue gas cleaning conditions (Srivastava et al., 2003), and temperature of the flue gas, which affects the removal process and mercury speciation (Wu et al., 2009).

In this study, the detailed activity data and end-of-pipe information in EDGARv4 allow for an appropriate allocation of specific mercury reductions by considering the average country-specific mitigation configurations for each power plant type; different reduction efficiencies were applied in EDGARv4 as described in Table S7 of the SI. Due to the absence of consistent information on removal efficiencies related to mercury species in the scientific literature, Hg removal efficiencies were applied to Hg^0, Hg^{2+}, and Hg-P in this study. According to the investigation of the SCR effects on mercury speciation under simulated conditions by Lee and Srivastava (2004), when 95% of Hg^0 is converted to Hg^{2+}, the splitting factors used in this study change from 50% Hg^0, 40% Hg^{2+}, and 10% Hg-P to 2.5% Hg^0, 87.5% Hg^{2+}, and 10% Hg-P, respectively. For example, applying this new splitting to the USA mercury emission fraction from power generation with an installed SCR system, the resulting emitted Hg^{2+} is 2.2 times higher than the EDGARv4 estimate. Moreover, the Hg^{2+} share of the total emitted country-wide mercury changes from 0.8% to 1.9%, which indicates that a more sophisticated representation of emission controls is needed.

2.2. Gridding

Given the local scale effects of some forms of mercury, special attention is given to the spatial distribution of emissions. The default EDGARv4 population proxy data (CIESIN, 2010), complemented with urban and rural population in-house EDGARv4 proxy data, were used to distribute combustion-related emissions from residential and industrial activities, and partially, for the solid waste incineration sector. For Europe, the solid waste incineration sector includes waste incinerator locations provided in the European Pollutant Release and Transfer Register database (E-PRTR) (EPRTRv4.2, 2012). For other sectors, point source data for power plants, industrial factories, and gold and mercury mines were used. Table S8 of the SI lists the proxy data used to distribute the mercury emissions in this study.

Emissions in EDGARv4 are calculated as country-wide totals and are distributed on 0.1° × 0.1° resolution gridmaps (bottom left corner type; emissions are allocated to latitude–longitude points, which correspond to the coordinates of the bottom left corners of the cells where the emissions are distributed) using the following equation:

$$EM_{cell,i,Hg} = EM_{C,i,Hg} * {}^{PROXY_{cell,i,Hg}}\Big/_{PROXY_{C,i,Hg}} \quad (3)$$

where C and i represent the country and the activity sector for which the emissions are distributed, respectively, $EM_{cell,\ i,Hg}$ is the emitted mercury inside the cell, $EM_{C,\ i,Hg}$ is the total emitted mercury for sector i in country C, $PROXY_{cell,\ i,Hg}$ is the proxy in the cell that is associated with the emitted mercury (e.g., population) and $PROXY_{C,\ i,Hg}$ is the proxy associated with the total emitted mercury in country C (e.g., population of country C).

When a cell belongs to more than one country, a surface-weighted percentage is calculated for each country. For cells containing sea areas, all emitted mercury in the cell is allocated to the adjacent countries except for costal fishing fuel combustion; maritime boundaries are considered for this emission source. A detailed description of the EDGARv4 gridding methodology is given in Janssens-Maenhout et al. (2013).

The new and updated proxy data and recent improvements in the EDGARv4 gridding methodology enhance the evaluation of local- and regional-scale effects of pollutants.

2.3. GEOS-Chem model

GEOS-Chem (version 9-01-03) is a global chemical transport model for atmospheric composition (www.geos-chem.org). The global mercury simulation of GEOS-Chem is described and evaluated in Selin et al. (2007, 2008) and Strode et al. (2007), with updates by Holmes et al. (2010), Soerensen et al. (2010) and Amos et al. (2012). The model includes a 3-D atmosphere, a 2-D surface-slab ocean and a 2-D terrestrial reservoir. Atmospheric redox chemistry follows Holmes et al. (2010), including the oxidation of Hg^0 by Br atoms and the photoreduction of Hg^{2+} and Hg-P in liquid cloud droplets. In this study, a GEOS-Chem model simulation with the EDGARv4 anthropogenic emissions inventory is performed from 1979 to 2008, which is the full range of meteorological years available for GEOS-Chem; in addition, observational data are not available to constrain pre-1996 atmospheric concentrations and wet deposition. The model is driven by Modern Era Retrospective-analysis for Research and Applications (MERRA) assimilated meteorological data from the Global Modelling and Assimilation Office Goddard Earth Observing System, which are produced at 0.5° × 0.667° horizontal resolution; these data are downgraded to a resolution of 4° × 5° for input into the GEOS-Chem model. The time-variant subsurface ocean mercury concentrations in the North Atlantic Ocean during the period 1990–2008 that are described in Soerensen et al. (2012) are applied; concentrations are held constant at their 1990 levels beginning in 1979. We do not include the in-plume reduction of oxidised mercury emitted from coal-fired power plants (Zhang et al., 2012b).

Modelled TGM concentrations are compared with available observations of TGM or GEM in North America from the CAMNet (CAMNet, 2012) and NADP/AMNet (NADP/AMNet, 2012) networks, in Europe from the EMEP network (EMEP, 2012) and at several individual sites, such as in Asia (Fu et al., 2012; MOE/Japan, 2013; Müller et al., 2012; Slemr et al., 2011). Because the contribution of GOM in TGM in remote surface air is very small (Lan et al., 2012; Temme et al., 2002), we do not distinguish between GEM and TGM in this paper unless indicated otherwise. The modelled total mercury (Hg^{2+} and Hg-P) wet deposition fluxes are compared with observations from the NADP/MDN (NADP/MDN, 2012) and EMEP networks. Instruments for high-frequency TGM concentration measurements (primarily Tekran Automated Ambient Air Analysers, Tekran Inc., Toronto, Canada) became available in the mid-1990s; these instruments were subsequently used at a few sites in North America and Europe. High-frequency TGM data were not available with a broader spatial coverage (e.g., Southern Hemisphere and East Asia) until approximately 2007. Similarly, only limited wet deposition flux data are available for before the mid-1990s. Therefore, we conduct model-to-observation comparisons for two periods: present day (2006–2008) and long term (1996–2008).

3. Results

3.1. EDGARv4 mercury emissions inventory: historical global trend and ex-post mercury mitigation assessment

According to EDGARv4, the amount of global emitted mercury was 1287 tonnes in 2008, which is 61% higher than in 1970, steadily increasing with an average of 1.3% annual growth (0.6% without including the artisanal and small-scale production sector). In this section, we identify the mercury species with major contributions to the global total mercury emissions (Fig. 1) and discuss contributions of the individual mercury species to the total emissions from the main sectors.

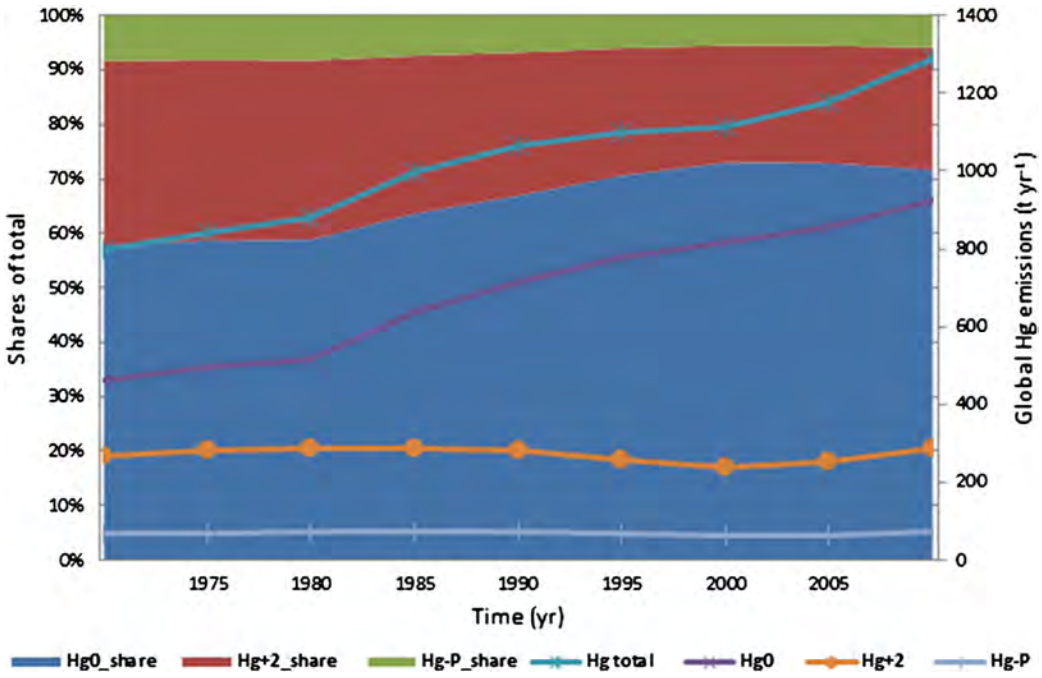

Fig. 1. EDGARv4 — shares (%) and global emissions of total mercury and mercury species [tonne/yr].

Hg^0 has the largest contribution to the total global mercury emissions, continuously growing with an average annual growth rate of 1.9% and accounting for 58% and 72% of the total emitted mercury in 1970 and 2008, respectively. Emissions of Hg^0 from artisanal and small-scale gold production, which contributed 19% and 43% of the total global Hg^0 in 1970 and 2008, respectively, determines the trend in global elemental mercury. Without included mercury emissions from artisanal and small-scale gold production, the average annual growth rate for emitted global Hg^0 would be substantially lower, amounting to only 0.9%.

The global mercury emissions of the other two species, i.e., Hg^{2+} and Hg-P, remained nearly stable over the period 1970–2008 and exhibited average annual growth rates of 0.2% and 0.3%, respectively. In 2008, these species accounted for 22% and 6% of the total global mercury emissions. Whereas the artisanal and small-scale gold production subsector almost exclusively drives the trend in Hg^0 and implicitly controls the total global mercury emission trend, Hg^{2+} and Hg-P are primarily driven by combustion processes. Combustion due to power generation and industrial, residential and waste activities comprised 78% of Hg^{2+} and 77% of Hg-P emissions in 2008.

Streets et al. (2011) found slightly different trends primarily due to the splitting factors used to estimate mercury species emitted from the power generation sector.

Generally, for the power generation sector, the trends in mercury emissions from gaseous and liquid fuel combustion follow the trends in activity data, representing 2.2% to 3.3% of the total global mercury emissions from this sector, respectively. However, solid fuel combustion remains responsible for the remaining mercury emission, varying from 97.8% to 96.7% of the total global mercury emissions from combustion in power generation within the analysed period (1970–2008) (Fig. S6 of the SI); therefore, solid fuel combustion drives the trend in mercury emissions for this sector. Over the same period, the shift in fuels can be seen in Fig. S7 of the SI combined with fuel consumption, which increased globally by 243%, i.e., 3.4 times higher than in 1970. In 1970, the shares of solid, liquid and gaseous fuels were 56%, 24% and 20%, whereas in 2008, the shares changed to 62%, 7% and 30%, respectively.

Mercury emissions in the power generation sector are affected by implemented end-of pipe (EoP) measures, the fuel characteristics and type and the technology used for combustion. In this work, we evaluate the effects of EoP measures on total mercury emissions over 39 years. Beginning in the mid-1980s, a large-scale implementation of ESP can be observed, which was primarily followed by the introduction of low NO_x burners, FF, FGD, SCR, and combinations of these control devices. These measures were implemented more often after 2000. In this study, the removal efficiencies for mercury emissions (equal for all species as described in Section 2.1.3) of the existing mitigation measures, which primarily target PM, NO_x and SO_2 pollutants, are applied to the power generation sector. An example of control device implementation is provided in Fig. S8 of the SI for combustion of other bituminous coal in power generation-public electricity production.

Two scenarios of mercury emissions from coal combustion in power generation are examined: *S1* — the baseline scenario, which considers existing emission reductions by EoP measures allocated to each power plant type (Platts, 2006), and *S2* — an ex-post mitigation assessment scenario, which assumes that no EoP measures have been implemented. Fig. S9 of the SI illustrates the global mercury emissions in both scenarios. Although fuel consumption has increased, the associated mercury emissions exhibited only small changes. Globally, 46% of mercury emissions were avoided in 2008, which means that 303 tonnes of mercury were not emitted into the atmosphere because of the mitigation measures in the power generation sector implemented during the period 1970–2008.

Mercury emission reductions in power generation are additionally obtained from control devices that were previously implemented; these reductions are demonstrated in Fig. S10 of the SI, which shows emissions of SO_2 and NO_x combined with mercury emissions from coal combustion in this sector for the two scenarios.

Analogously, the chlor-alkali industry is also analysed. Chlorine is produced using three different technologies; amongst these technologies, mercury cells are of the highest concern. In the EDGARv4 database, mercury emissions from mercury cell technology in the chlor-alkali industry were very high in the 1970s, accounting for 13–15% of the total global mercury emissions. To improve the health conditions of the local environment, many countries either switched from mercury cell technology to diaphragm and membrane cell electrolysis and/or improved the mercury cell technology. Some countries phased out (e.g., Japan, Canada, and Australia) or diminished the use of mercury cell technology when producing chlorine and caustic soda (Fig. S11b of the SI). Based on emission improvements in Europe, the effects of technology improvements over this period for industrialised countries and for the rest of the world can be analysed by considering that the mitigation measures were implemented in those regions with a certain delay (based on expert judgement) compared to Europe. As a consequence of both phasing out and technology improvements, total mercury emissions from this sector decreased by 93%, reaching 7.2 tonnes in 2008 and avoiding the emission of 98.7 tonnes of mercury. The

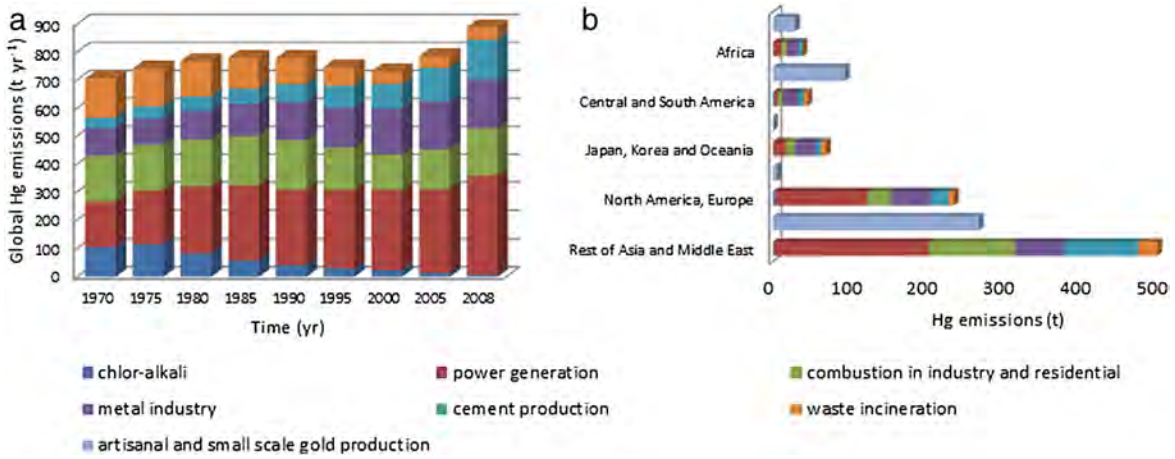

Fig. 2. Global mercury emissions: (a) Global mercury emission trends by sector (emissions from artisanal and small-scale gold production sector are not included) [tonne]. Note sectors are delineated from bottom of the bar to the top as chlor-alkali, power generation, combustion, metal industry, cement production, and waste incineration. (b) Sector-based mercury emission contribution by region [tonne] in 2008; artisanal and small-scale gold production is reported separately as the top bar for each region. (For interpretation of the references to colour in this figure, the reader is referred to the web version of this article.)

resulting pattern of mercury emissions in the chlor-alkali industry over 1970–2008 period is illustrated in Fig. S11a of the SI. Although the emissions from some of the facilities are missing due to a lack of information, we consider that 80% of the global emissions from the chlor-alkali industry, specifically from mercury cell technology, are captured in the EDGARv4 mercury emission inventory.

3.2. The trends and shares of mercury emissions by region and by sector

The global mercury emission trends during the period 1970–2008 for the main contributing sectors (waste incineration, cement production, metal and chlor-alkali industries, and combustion in manufacturing, residential and power generation) are illustrated in Fig. 2a; due to the large uncertainty, mercury emissions from artisanal and small-scale gold production (see Section 4.1) are not included in this analysis (here, global total means global total mercury without emissions from this sector). The global share of mercury emissions from the chlor-alkali industry drastically changed from 15% in 1970 to 1% in 2008. In the waste incineration sector, mercury emissions decreased by 68% for the same period, decreasing from a share of 20% to 5% of the global total. However, the emissions from combustion in industry and residential activities remained nearly unchanged. Increases in mercury emissions are observed in power generation, metal industry and cement production, with contributions to the global total changing from 23 to 40%, 14 to 20% and 5 to 16%, respectively. The increase in global mercury emissions after 2000 (excluding mercury emissions from artisanal and small-scale gold production) was driven primarily by the emission of the power generation and cement production sectors in China.

For 2008, Fig. 2b shows the mercury emission by sector and by region including emissions from artisanal and small scale gold production. The light blue bars illustrate the artisanal and small-scale gold production contribution to the total global mercury emissions by region. The share of mercury emissions from this sector is approximately 30.8%; 21% originates from the Rest of Asia and the Middle East (China included), 7% from Central and South America and 2% from Africa.

3.3. Gridded mercury emissions as input for chemical transport models

EDGARv4 provides global gridded mercury emissions for the period 1970–2008 on 0.1° × 0.1° resolution gridmaps; separate emissions are provided for Hg, Hg^0, Hg^{2+} and Hg-P. Because the mercury species are characterised by different reactivities, an important added value compared to earlier inventories is the high spatial resolution of the EDGARv4 mercury emission inventory and the relatively detailed proxy data used for the spatial distribution of emissions, which permits the inventory to be verified at relatively small spatial scales. Total mercury and individual mercury species are available as gridded emission maps and data files for each year (see the "Data availability" section). In Figs. S12 and S13 of the SI, the total mercury emission distributions on 0.1° × 0.1° resolution gridmaps are presented for 1970 and 2008 as an example, which show the areas of elevated mercury emissions for these years.

Fig. 3, which represents the difference between total mercury emissions in 2008 and 1970 aggregated to 1° × 1° resolution to better emphasise changes, shows that mercury emissions declined in the United States, EU27 and Japan primarily due to technology changes and mitigation measures in the chlor-alkali industry and combustion. Combustion in power generation and the increase in cement and non-ferrous metal production increased mercury emissions in China and India. During this period, gold production caused an increase in mercury emissions in South America and Indonesia and a decrease in Southern Africa.

3.4. Comparison of EDGARv4 mercury emissions with the UNEP — 2005 inventory

The widely used UNEP global mercury emission inventory for 2005 reports their best estimates from which a lower and upper limit of global mercury emissions can be derived; the UNEP estimates (uncertainty interval) and conservative estimates (no associated range) for selected sectors are presented in Table S9 of the SI. We compare this range with the EDGARv4 mercury emission estimates for 2005. A breakdown by sector for both the EDGARv4 and UNEP mercury emission inventories is presented in Fig. S14 (a, b) of the SI.

Here, Fig. 4 shows a comparison for 9 dominant sectors using aggregated data from UNEP study (UNEP, 2010), which can be coupled with the more detailed EDGARv4 activities. As a consequence, mercury emissions from "other waste" (74 tonnes) and "other sectors" (62 tonnes) in the UNEP emission inventory and "agricultural waste burning" (4.4 tonnes) in EDGARv4 are not included in this analysis.

The iron and steel sector contributed 53.3 tonnes of mercury to the total global mercury emissions in 2005, which is close to the UNEP emission for this sector. Moreover, the EDGARv4 mercury emissions from combustion in power generation and the industry sector are estimated to be 374.7 tonnes, reaching 631.6 tonnes when the mercury removal by end-of-pipe measures is not considered; these values are within the UNEP mercury emission range, which may indicate that the UNEP maximum range primarily refers to the hypothetical case that no abatement techniques are installed in the power generation sector. Mercury emissions from large-scale gold production (64.3 tonnes), cement production (120 tonnes) and waste incineration (42 tonnes) are close to the UNEP minimums. Mercury emissions from non-ferrous metal

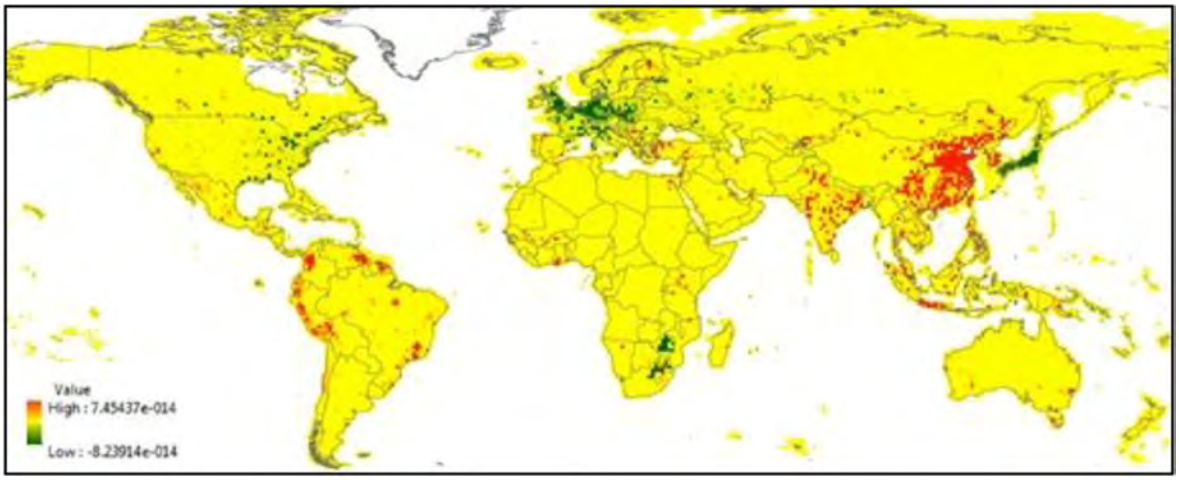

Fig. 3. The difference between total mercury emissions in 2008 and 1970 aggregated to 1° × 1° resolution [kg/m^2/s].

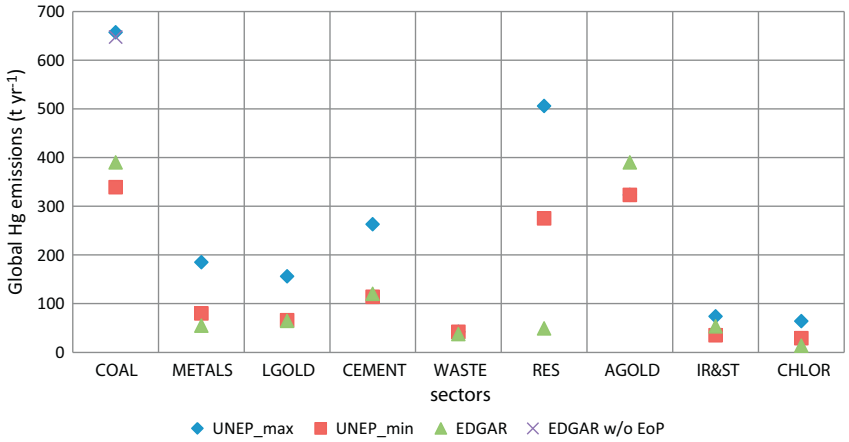

Fig. 4. EDGARv4 (this study) vs. UNEP (UNEP, 2010) comparison of global mercury emissions for 2005 aggregated for 9 dominant sectors: 1. COAL - Coal combustion in power generation and industry, 2. METALS - Non-ferrous metals (other), 3.LGOLD - Large scale gold production, 4. CEMENT - Cement production, 5. WASTE - Waste incineration, 6. RES - Residential and other combustion, 7. AGOLD - Artisanal and small-scale gold production, 8. IR&ST - Iron and steel, 9. CHLOR - Chlor-alkali industry.

production (other) are 54.5 tonnes, which is 32% lower than the UNEP minimum. EDGARv4 mercury emissions from the chlor-alkali industry are 16 tonnes less than the UNEP minimum, while emissions from artisanal and small-scale production are 21% higher than the UNEP mercury emissions. Mercury emissions aggregated as residential and other combustion (key sector 6) are largely below the UNEP range, i.e., 210 tonnes less than the UNEP minimum.

From Fig. 4 and Table S9 of the SI, the emissions reported by EDGARv4 are consistent with the UNEP mercury emission inventory for some sectors; however, for the dominant selected sectors, the UNEP total emissions are 1785 tonnes (1285–2270 tonnes), while the EDGARv4 total emissions are 1172 tonnes (1429 w/o EoP measures), which is close to the lower bound of the UNEP best estimate for mercury emissions.

A complete explanation of the differences in the UNEP and EDGARv4 mercury emission inventories could be found by further exploring the approaches, activity data and emission factor data sources used in each inventory; this is not the goal of this paper. However, some qualitative remarks can be presented. The consistency in 2005 for some sectors, such as artisanal and small-scale gold production and large-scale gold production, is because the same emission factors and activity data sources are used in both emission inventories. Moreover, the USGS activity data for non-ferrous metals (other), cement and iron and steel production produced relatively good agreement in the results, while the lower mercury emissions in EDGARv4 can be explained by differences in emission factors, e.g., for cement production, UNEP uses $EF_{UNEP} = 0.1$ g/tonne$_{cement,}$ whereas EDGARv4 uses $EF_{EDGAR} = 0.063$ g/tonne$_{clinker}$ together with the clinker percentage for each country to derive country-specific emission factors for this sector. The largest difference occurs in the residential sector, which can be partially explained by the differences in emission factors used in the two inventories; more specifically, EF_{UNEP} is approximately 2.5 times higher than the emission factor applied in EDGARv4 for the predominant technologies and coal types used for combustion in the residential sector.

3.5. Evaluation of the EDGARv4 mercury emission inventory with the GEOS-Chem global simulation

As mentioned in Section 2.3, due to the availability of observational data, model-to-observation comparisons are analysed for two periods: present day (2006–2008) and long term (1996–2008).

3.5.1. Comparison in the present day period (2006–2008)

A scatter plot comparing the modelled to the observed TGM concentrations is provided in Fig. 5(a). For all sites, the discrepancies between the modelled and observed TGM concentrations are less than a factor of

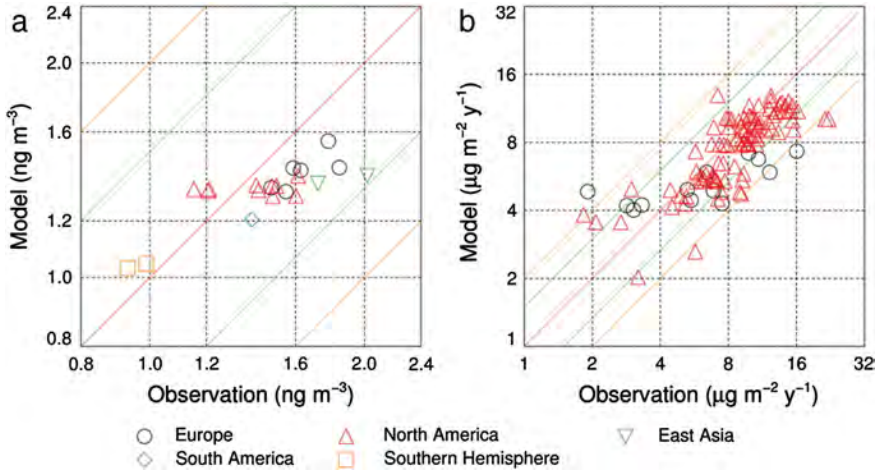

Fig. 5. Scatter plots comparing model output to observations during the period 2006–2008 for (a) TGM concentrations and (b) total mercury wet deposition fluxes. The red lines indicate the 1:1 ratio; the green and orange lines correspond to deviation factors of 1.5 and 2, respectively. (For interpretation of the references to colour in this figure legend, the reader is referred to the web version of this article.)

1.5. Regionally, the model overestimates TGM levels at the two sites in the Southern Hemisphere by 8% on average and underestimates TGM levels at most sites in the Northern Hemisphere by 6% in North America and by 14% in Europe. The modelled spatial distribution of TGM in surface air is shown and compared to observations in Fig. S15 of the SI. The modelled TGM distribution exhibits a pronounced interhemispheric gradient; lower concentrations (<1.2 ng m^{-3}) are found in the Southern Hemisphere, which is consistent with the limited observational dataset. Elevated TGM levels are both observed and modelled in East Asia, where the largest anthropogenic emission sources are located.

As shown in Fig. 5(b), the discrepancy between the modelled and observed wet deposition fluxes is within a factor of 2 for most sites. On average, the model underestimates the wet deposition fluxes by 14% and 25% in North America and Europe, respectively. Fig. S16 of the SI presents the modelled and observed spatial distributions of the wet deposition fluxes in North America and Europe. In general, the model predicts high wet deposition fluxes in regions with intensive anthropogenic emissions, reflecting the local deposition of Hg^{2+} and Hg-P emissions (Holmes et al., 2010). The observed wet deposition fluxes are elevated in central Europe and exhibit a poleward decrease that is larger than the model prediction. The model underestimates both TGM concentrations and wet deposition fluxes more strongly in Europe compared to North America.

3.5.2. Comparison in the long-term period (1996–2008)

Long-term TGM concentration measurements with known data quality are available at only a few sites that are operated by different laboratories (Slemr, 2003). A generally good agreement for TGM measurements from the different laboratories was found in several field intercomparison campaigns (Ebinghaus et al., 1999; Munthe et al., 2001). For example, in a four-day field intercomparison experiment, the average TGM concentrations reported by four laboratories using Tekran automated instruments varied from 1.69 ng m^{-3} to 1.82 ng m^{-3} (Ebinghaus et al., 1999). This good agreement warrants comparability of the signal and trend in Fig. 6.

Fig. 6 shows the observed and modelled concentrations of annual average TGM during the period 1996–2008 at three background sites: Mace Head (Ireland), Kejimkujik (Canada), and Cape Point (South Africa). The temporal trends (mean ± standard error) calculated from the least-square fits are also presented. A significantly decreasing trend in the TGM concentration was found at Mace Head and Cape Point in both the observations and model output at the 0.05 significance level, while a significant decreasing trend was observed but not simulated for Kejimkujik. In the model, most of this decrease is attributed to the decreasing mercury emissions from the ocean as a result of declining subsurface ocean Hg concentrations in the North Atlantic Ocean (Fig. S17 of the SI). This decreasing trend may be due to decreased riverine and wastewater inputs of Hg in ocean margins (Soerensen et al., 2012). Riverine and wastewater inputs peaked in the 1970s. Moreover, potentially because of regulations in mercury-related industry sectors and products since the 1970s, the input fluxes decreased and produced lower subsurface ocean Hg concentrations. The declining subsurface ocean Hg concentrations resulted in a decrease of 1300 tonnes in the modelled global ocean emissions during the period 1990–2008. Over the same period, the anthropogenic emissions only increased by ~200 tonnes based on the EDGARv4 inventory. Therefore, although anthropogenic emissions have been increasing, the GEOS-Chem model can still reproduce the observed decreasing trend in TGM concentrations.

Fig. 7 shows the modelled and observed wet deposition fluxes of total mercury over North America (14 sites) and Europe (5 sites) during the period 1996–2008. Sites with data available for at least 75% of a month are used. In general, the model reproduces the decreasing trends in the wet deposition fluxes for both regions. The modelled trend of -0.68 ± 0.19 ng m^{-2} d^{-1} y^{-1} for North America is not significantly different than the observed trend of -0.49 ± 0.30 ng m^{-2} d^{-1} y^{-1}, which is also the case for Europe.

3.6. Uncertainties

The uncertainties in both the activity data and emission factors used in the EDGARv4 mercury emission inventory are estimated using the default methodology recommended by IPCC (2006) with the lower and upper bounds of the 95% confidence interval from EMEP/EEA (2009) expressed as a percent relative to the mean for emission factors. The estimated uncertainty when combining the cement production, metal industry, combustion and waste incineration sectors ranges from −26 to +33% for OECD24 (24 OECD members in 1990) and Economies in Transition (EIT — Russia Federation, Ukraine and other eastern European countries) countries and −33 to +42% for Non-Annex I (defined in UNFCCC) countries. Table S10 of the SI shows the range in emissions by sector for 2008. However, the uncertainty in the mercury emission inventory is expected to be much higher because it is difficult to calculate the uncertainty in the activity data for artisanal and small-scale gold production resulting from the lack of official statistics in most countries, and also because there are large uncertainties in mercury emission factors associated with gold, mercury and chlorine production. In addition, due to scarce information, uncertainties in the reduction efficiencies for the different mercury species of control devices in the power generation sector are not considered. Although estimates are calculated with high precision, the contribution to emissions from highly uncertain sectors (e.g., artisanal and small-scale gold

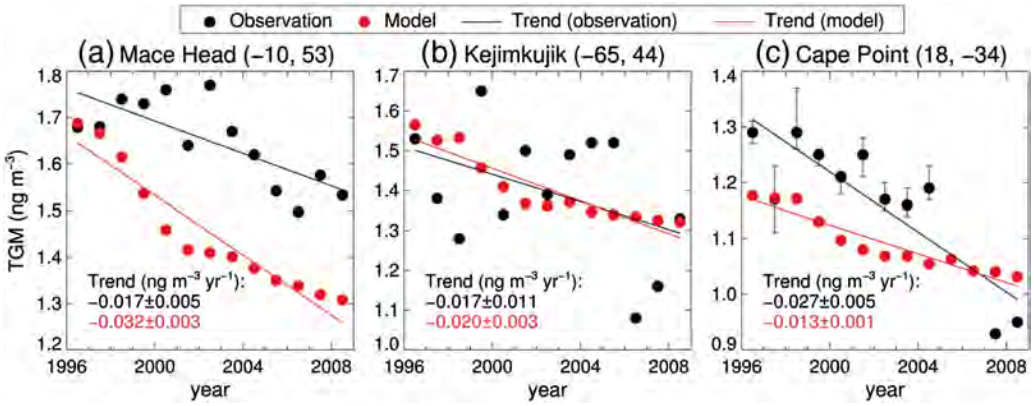

Fig. 6. Time series of the observed and modelled TGM concentrations with least-square fit trend lines at three background sites (longitude, latitude). For the observations, the circles and bars represent the annual medians and the 95% confidence intervals of the medians, respectively. For the model output, the circles represent the annual means. Only baseline observational data were used for Mace Head (Ebinghaus et al., 2011). TGM was manually measured at Cape Point until 2004; all other measurements were made using an automated method (Slemr et al., 2011). The median confidence intervals for the automated measurements are smaller than the circles.

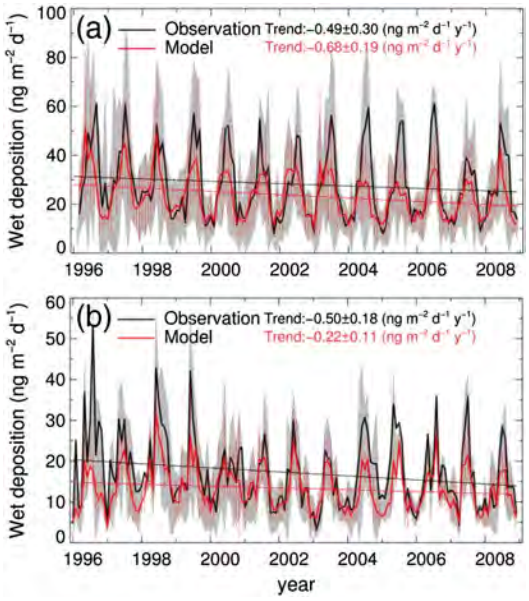

Fig. 7. Comparison between the modelled (red curve) and observed (black curve) monthly mean wet deposition fluxes of total mercury over (a) North America and (b) Europe during the period 1996–2008. The model results are sampled at the observation sites. The grey shaded regions and red error bars indicate standard deviations calculated from the observed and modelled monthly means of the individual sites, respectively. Regressions and temporal trends for both the model results and observations are also depicted. (For interpretation of the references to colour in this figure legend, the reader is referred to the web version of this article.)

production) and the high contribution from developing countries increase the uncertainty range with time.

Furthermore, caution is required when interpreting results of the model-to-observation comparisons. Uncertainties exist in both the observations and model results; several important uncertainties are described below. Intercomparison experiments have suggested that uncertainties in both the observed TGM concentrations and wet deposition fluxes are approximately 10% (Lindberg et al., 2007; Ebinghaus et al., 1999; Prestbo and Gay, 2009). The coarse horizontal and vertical resolutions (4° × 5°, 47 vertical layers) of the model lead to mismatch errors. For example, the global model does not capture the observed high wet deposition fluxes along the USA Gulf Coast, whereas a nested model with a finer (1/2° × 2/3°) horizontal resolution performs much better (Zhang et al., 2012b). Atmospheric redox chemistry of mercury, which can strongly affect its global distribution, is still poorly understood (Pirrone et al., 2013). Very limited observations are available in the Southern Hemisphere and in the regions where anthropogenic emissions are most important (e.g., East Asia).

4. Discussion

This section focuses on the mercury emissions from artisanal and small-scale gold production, which has an important share in the global total mercury emissions and consequently produces large uncertainties in the EDGARv4 inventory. Insight on the regional importance of sectoral emissions is also given and discussed in 24 regions of the world (listed in Table S11 of the SI), and important findings regarding the evaluation of this inventory using atmospheric transport and chemistry modelling and available ground measurements are presented herein.

4.1. Large uncertainty in artisanal and small-scale gold production; substantial differences when using a poverty-based approach

With a 30.8% contribution to the total global mercury emissions in 2008, special attention should be given to estimating mercury emissions from artisanal and small-scale gold production. As mentioned in Section 2.1.1, due to no official reporting of gold production or mercury used for amalgamation, the trends in large-scale gold production were applied to the inventory developed by Telmer and Veiga (2008) to estimate the mercury used in artisanal and small-scale gold production since 1970; the gold market demand was considered to be the only driver of mercury emissions in this study. However, other drivers, such as mercury price, poverty, technology improvement and the presence and effectiveness of legislation, could also affect mercury emissions from this activity.

As an alternative to the approach used in EDGARv4, here we made the assumption that the poverty state in some countries that are rich in gold ore stimulated artisanal and small-scale gold production, which is associated also with the low price of mercury caused at least partially by the phasing out of chlor-alkali mercury cell technology (Maxson, 2005; UNEP, 2006; USGS, 2013). Mercury emissions generated by this "dirty" activity, which has harmful effects on health even though it is an important source of income in countries with very poor people, were estimated using the GINI index as a measure of poverty and inequality (Kamdem, 2012). Due to scarce GINI index data, only the average values for 1995–1999, 2000–2004 and 2008 and for 52 out of 73 countries with artisanal and small-scale gold production activity data in 2008 were calculated using the WB (2013) statistics.

For 40 countries a good correlation has been found between activity data as mercury consumption in artisanal and small-scale gold production in 2008 and GINI index. For these countries, the polynomial regression function (based on the year 2008) presented in Fig. S18 of the SI was used to estimate the activity data for artisanal and small-scale gold production since 1995.

As in the EDGARv4 approach, the emission factor used to calculate mercury emissions was 0.4 ktonnes mercury emission/ktonne of mercury used in artisanal and small-scale gold production. The emissions from the two approaches are illustrated in Fig. S19 of the SI. A comparison suggests that when poverty is the driver, mercury emissions, especially Hg^0, are 40% higher for 1995–1999 and 36% higher for 2000–2004 than when the gold market demand is assumed to be the driver. However, this substantial change should be considered with caution because the mercury emissions of the countries included in this analysis account for only 30% of the total mercury emissions from this sector.

Recent estimates from the Artisanal Gold Council (AGC, 2010), which provide new insight into this issue, indicate that the atmospheric emissions from artisanal and small-scale gold production may be much higher in 2010 compared to the level estimated by Telmer and Veiga (2008) for 2008 (Table S12 of the SI); this information will be included in EDGAR mercury time series extension to 2010.

4.2. Mercury emission magnitude by region

Predominant emitting sectors are illustrated in Fig. 8 with a finer breakdown of mercury emissions by region for 2008; this analysis also includes large countries. Mercury emissions were aggregated for 24 world regions as defined in the IMAGE model (Bouwman et al., 2006). The mitigation potential of each region is highlighted by the contributions (%) of the main sectors to the total regional mercury emissions. Emissions from the power generation sector are dominant in the United States, OECD Europe, Central Europe, and India, whereas emissions from artisanal and small-scale gold production are important sources in China+, Indonesia+, Rest of South America, Southeastern Asia and Brazil (these regions are defined in Table S11 of the SI). The metal industry is also a substantial source of mercury in many regions, e.g., Japan, Korea, Oceania, Canada, and OECD Europe.

The region with the greatest share (40%) of the global total mercury emissions in 2008 is China+, which is illustrated in Fig. 8 (labelled [4]); within this region, emissions from artisanal and small-scale gold production represent 35%, power generation represents 26%, combustion in industry and buildings 15%, and cement production contributes

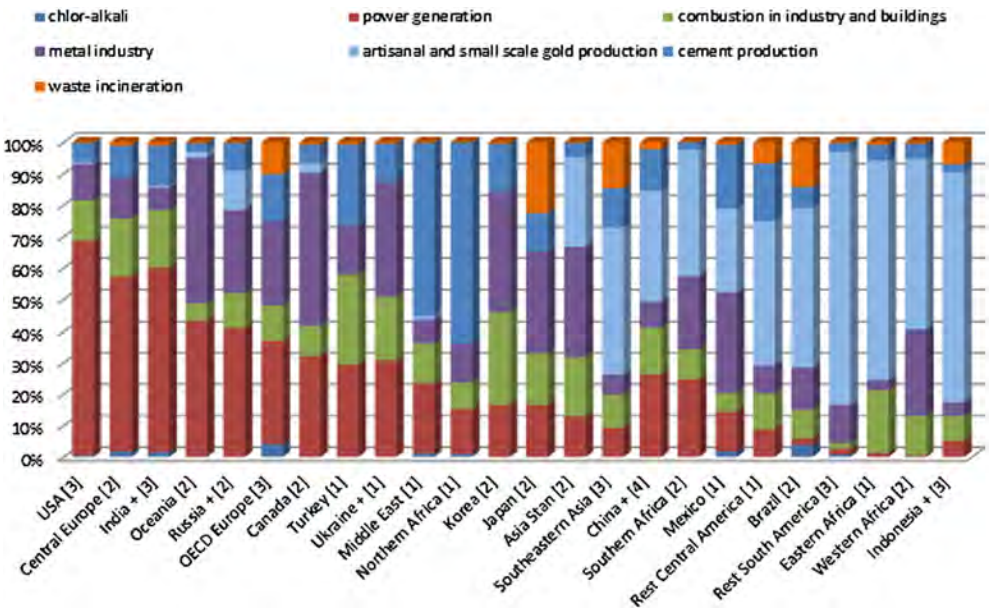

Fig. 8. Mercury emissions sector contributions (%) by region/country in 2008. The share in global total mercury emission for each region/country is also indicated with [1], [2], [3] and [4] labels that represent shares <1%, in the range 1–3% and 3–7%, and a share of 40%, respectively. Note bars include from bottom to the top sectors from top left to bottom right.

13%. China +, which was the largest contributor to the global mercury emissions in 2008, is followed by the Rest of South America, the United States, India, Indonesia +, and OECD Europe, which accounted for 5 to 7% each of the global total mercury emissions. The rankings of the 24 regions are provided in Fig. 8 using labels from [1] to [4].

This regional mercury emission contributions snapshot for the year 2008 combined with the results from trend analysis show that artisanal and small-scale gold production is the most significant source of mercury to the atmosphere. Therefore, mitigation policies applied to this sector will have the largest impact on global mercury emission; these findings are consistent with Minamata convention provisions. Moreover, based on the mercury mitigation achievements highlighted in the ex-post analysis in Section 3.1 and this regional emission insight we also conclude that in power generation sector important mercury reduction can be performed, for emerging economies in particular.

4.3. Further improvements based on the GEOS-Chem simulations

In general, the GEOS-Chem model simulation using the EDGARv4 inventory successfully reproduces both spatial and temporal variations in the observed TGM concentrations and wet deposition fluxes of total mercury. However, some discrepancies between the model and observations exist and suggest possible areas of further improvements and investigations. For example, the observed wet deposition fluxes are elevated in Central Europe and exhibit a larger poleward decrease than predicted by the model, possibly suggesting an underestimate of Hg^{2+} and Hg-P emissions in the EDGARv4 inventory during the period 2006–2008 or uncertainties in the speciation of emitted mercury. The model underestimates both TGM concentrations and wet deposition fluxes more strongly in Europe compared to North America, which may suggest that mercury emissions from Europe may be relatively underestimated during this period. The modelled wet deposition trends of -0.68 and -0.22 ng m^{-2} d^{-1} y^{-1} for North America and Europe during the period 1996–2008 are slightly different from the observed trends of -0.49 and -0.50 ng m^{-2} d^{-1} y^{-1}. The different trends may suggest different emission reduction rates for sources of Hg^{2+} and Hg-P. It is also possible that the removal efficiencies of emission control technology for different mercury forms have changed with time.

5. Conclusions

The goal of this work was to derive global and regional mercury emission trends from 1970 to 2008 using the EDGARv4 global emission database technology-based approach and to evaluate the consistency of this emission inventory with concentration and deposition flux measurements using the GEOS-Chem global 3-D mercury model. This paper contributes to the understanding of the geospatial and temporal patterns in mercury emissions, by compiling a global emissions database for the major Hg species using consistent international statistics and open source data. Compared to earlier studies, we provide an improved methodology to derive a historical mercury emission trend for nearly four decades and analysed the effects of past policies that aimed for high implementation rates of clean technologies in industry (e.g., chlor-alkali/power) on a global scale; a model evaluation of this emission inventory provides additional understanding of emission processes.

A mercury emission inventory was produced across all world countries, by primarily applying EMEP/EEA (2009) and US EPA/AP42 emission factors, combined with international activity statistics and regional technology-specific abatement measures. In the power generation sector, air pollution mitigation policies exhibited an emission reduction of 46% by implemented end-of-pipe measures which are approximately globally offset by the increase in fuel consumption over the period 1970–2008. In this sector, mercury emission reductions are additionally obtained from the control devices already implemented that were primarily intended to reduce PM, NO_x, and SO_2 (Fig. S10 of the SI). In the chlor-alkali industry, mercury emissions decreased by 93% due to structural technology changes. The improved technologies and mitigation measures in these sectors accounted for 401.7 tonnes of avoided mercury emissions in 2008.

One of the most uncertain sectors for mercury emissions is artisanal and small-scale gold production. Two independent methodologies to assess emissions and trends from this sector and to provide insight on the associated uncertainty were used. Due to the lack of officially reported information regarding artisanal and small-scale gold production, trends in large-scale gold production were used to derive activity data for this sector; the gold market demand was considered to be the main driver for this sector. However, poverty is another important

factor that affects the evolvement and implicit emission changes in this sector. Using the GINI (inequality) index as an indicator of poverty, we demonstrate that higher emissions could be estimated using an equally uncertain methodology. This investigation shows the role of emission estimation approaches and suggests that the trend in global mercury emissions, especially Hg^0, is sensitive to the emission estimation approach and uncertainty that is applied to this particular sector due to its important share in the total global mercury emissions.

In 2008, China + exhibited the largest contribution (40%) to the global total mercury emissions, followed by the Rest of South America, the United States, India, Indonesia +, and OECD Europa, each with shares of 5 to 7%. Given the variation in the contributing sectors amongst the different regions, no unique global measure can be effective, since each region has its sector(s) of concern. We identified the proportion of each sector to the total mercury emissions per region/large country in 2008. Power generation is dominant in the United States, Central Europe and India, whereas artisanal and small-scale gold production has a large contribution in China +, Indonesia, Western Africa, and South America.

Anthropogenic mercury species should be addressed with the necessary regional differentiation when assessing their effects; therefore, high-resolution spatial information is needed. EDGARv4 provides gridded total mercury and mercury species emissions on $0.1^\circ \times 0.1^\circ$ resolution gridmaps for each year in the period 1970–2008 and for each disaggregated sector. New and updated proxy data (CARMAv3.0, 2012; CIESIN, 2010; USGS, 2010) are used to distribute mercury emissions on global gridmaps.

The EDGARv4 mercury emission inventory and its trends were evaluated using the GEOS-Chem global 3-D model and available ground measurements. The model successfully reproduced both spatial and temporal variations in wet deposition fluxes and TGM concentrations. However, some discrepancies between the model results and observations indicate possible underestimates of Hg^{2+} and Hg-P for Central Europe during the period 2006–2008. Differences in modelled and observed trends in the wet deposition fluxes over North America and Europe during the period 1996–2008 also suggest the presence of differences in emission reductions for Hg^{2+} and Hg-P in developed regions. However, there were no systematic over/or underestimates of these trends at all stations.

An important aspect of this database is that mercury emission trends were largely determined by trends from only a few point sources. The current relatively low-resolution version of the GEOS-Chem model used in this study to evaluate whether we can reproduce large scale features and temporal trend of atmospheric observations was not capable of exploiting the spatially resolved information on location and trends that are included in EDGARv4. This 0.1×0.1 high-resolution information may potentially shed light on discrepancies near these point sources. Utilisation of high temporal/spatial information in an inverse modelling context could possibly provide a step forward.

Several uncertainties that are intrinsic to all aspects of the mercury cycle included in the model and a lack of observations outside of Europe and North America preclude drawing firm conclusions on the accuracy of our global estimates. However, model comparisons illustrate that the emission inventory is plausible and shows realistic temporal trends and spatial distributions consistent with current understanding of the mercury cycle. Nevertheless, new process and statistical findings and high quality observational data will be very beneficial for future EDGARv4 improvements.

Importantly, the GEOS-Chem mercury modelling suggests the substantial role of declining ocean re-emissions in explaining the observed negative trends at 1 southern hemisphere and 2 northern hemisphere background stations. Because our work shows that global emissions continue to increase, the point at which the ocean may become an increasing source again and the corresponding future levels of anthropogenic and ocean concentrations and associated health and ecosystem effects remain uncertain. This concern was raised by Amos et al. (2013), who posed that aggressive global mercury emission reductions are needed to stabilise ocean mercury concentrations at their current levels.

6. Data availability

EDGARv4.tox1 mercury emissions are disaggregated by sector and gridded emission data files are provided in two formats: netCDF (in $kg/m^2/s$) and .txt (in t/cell) on http://edgar.jrc.ec.europa.eu/edgar_v4tox1/index.php.

Conflict of interest

There is no conflict of interest of any type regarding this paper as all the authors declared.

Acknowledgments

The views expressed here are purely those of the authors and may not be regarded as an official position of the European Commission or of any other research institutions.

The authors would like to thank the anonymous reviewers for their valuable comments and suggestions to improve the quality of the paper.

SS and NES acknowledge support from the U.S. National Science Foundation Atmospheric Chemistry Program (Grant #1053648).

Appendix A. Supplementary data

Supplementary data to this article can be found online at http://dx.doi.org/10.1016/j.scitotenv.2014.06.014.

References

ABICLOR. Statistics Yearbooks: BRAZIL_relatório_2004_A.pdf, BRAZIL_2005_Anuário.pdf, BRASIL_relatorio_2006.pdf, BRAZIL_2007_relatorio.pdf, BRAZIL_2008_Abiclor.pdf, BRAZIL_2010_Relatorio.pdf. Brazilian chlor-alkali industry, [info retrieved from http://www.abiclor.com.br/ [on 15 December 2011]], 2004, 2005, 2006, 2007, 2008, 2010.

ACAP. Arctic mercury releases inventory. Copenhagen: Arctic Council Action Plan to Eliminate Pollution of the Arctic (ACAP) & Danish Environmental Protection Agency; 2005.

AGC. Global database on mercury emissions from artisanal and small scale mining (ASGM). Artisanal Gold Council; 2010 [info retrieved from www.mercurywatch.org [on 15 October 2013]].

AMAP. AMAP assessment 2011: mercury in the Arctic. Oslo, Norway: Arctic Monitoring and Assessment Programme (AMAP); 2011 [xiv + 193 pp.].

AMAP/UNEP. Technical background report to the global atmospheric mercury assessment. Arctic Monitoring and Assessment Progamme/UNEP Chemicals Branch; 2008.

Amos HM, Jacob DJ, Holmes CD, Fisher JA, Wang Q, Yantosca RM, et al. Gas–particle partitioning of atmospheric Hg(II) and its effect on global mercury deposition. Atmos Chem Phys 2012;12:591–603.

Amos HM, Jacob DJ, Streets DG, Sunderland EM. Legacy impacts of all-time anthropogenic emissions on the global mercury cycle. Global Biogeochem Cycles 2013;27:410–21.

Ayers R. The life-cycle of chlorine, part I: chlorine production and the chlorine–mercury connection. J Ind Ecol 1997;1:81–94.

Bouwman AF, Kram T, Goldewijk KK. Integrated modelling of global environmental change. An overview of IMAGE 2.4, MNP publication number 5001 10002/2006. Bilthoven: Netherland Environmental Assessment Agency; 2006.

CAMNet. Canadian atmospheric mercury network. Canada: Environment; 2012 [http://www.on.ec.gc.ca/natchem/Login/Login.aspx].

CARMAv3.0. Carbon monitoring for action. CARMA; 2012 [info retrieved from http://carma.org/blog/carma-notes-future-data/].

CIESIN. Global rural–urban mapping project (GRUMP), v1. CIESIN; 2010 [info retrieved from http://sedac.ciesin.columbia.edu/data/set/grump-v1-population-density].

Ebinghaus R, Jennings SG, Schroeder WH, Berg T, Donaghy T, Guentzel J, et al. International field intercomparison measurements of atmospheric mercury species at Mace Head, Ireland. Atmos Environ 1999;33:3063–73.

Ebinghaus R, Jennings SG, Kock HH, Derwent RG, Manning AJ, Spain TG. Decreasing trends in total gaseous mercury observations in baseline air at Mace Head, Ireland from 1996 to 2009. Atmos Environ 2011;45:3475–80.

EMEP. European monitoring and evaluation programme: co-operative programme for monitoring and evaluation of the long-range transmission of air pollutants in Europe. EMEP; 2012 [http://www.nilu.no/projects/ccc/emepdata.html].

EMEP/EEA. EMEP/EEA CORINAIR emission inventory guidebook. Technical report No 9/2009. European Environment Agency; 2009 [http://www.eea.europa.eu/publications/emep-eea-emission-inventory-guidebook-2009].

EPRTRv4.2. The European pollutant release and transfer register. EPRTR; 2012 [info retrieved from http://www.eea.europa.eu/data-and-maps/data/member-states-reporting-art-7-under-the-european-pollutant-release-and-transfer-register-e-prtr-regulation-6].
Eurochlor. Mercury process for making chlorine. Eurochlor; 1998 [info retrieved from http://www.chem.unep.ch/mercury/2003-ngo-sub/Eurochlor/Mercury%20process%20for%20making%20chlorine.pdf [on 15 December 2011]].
FAO. Food and Agricultural commodities production. FAOSTAT. [info retrieved from http://databank.worldbank.org/data/home.aspx], 2011.
Foerter DC, Whiteman CS. Opinion of the Institute of Clean Air Companies (ICAC) concerning mercury control technologies. ID No. OAR-2002-0056. ICAC; 2005 [info retrieved from http://c.ymcdn.com/sites/www.icac.com/resource/resmgr/MercuryControl_PDF%27s/hgcontrol010305.pdf [on 15 October 2013]].
Fu XW, Feng X, Liang P, Deliger, Zhang H, Ji J, et al. Temporal trend and sources of speciated atmospheric mercury at Waliguan GAW station, Northwestern China. Atmos Chem Phys 2012;12:1951–64.
Gustin MS, Huang JY, Miller MB, Peterson C, Jaffe DA, Ambrose J, et al. Do we understand what the mercury speciation instruments are actually measuring? Results of RAMIX. Environ Sci Technol 2013;47:7295–306.
Holmes CD, Jacob DJ, Corbitt ES, Mao J, Yang X, Talbot R, et al. Global atmospheric model for mercury including oxidation by bromine atoms. Atmos Chem Phys 2010;10:12037–57.
HTAP. Hemispheric transport of air pollution, part B: mercury. HTAP; 2010 [http://www.htap.org/publications/2010_report/2010_Final_Report/HTAP%202010%20Part%20B%20110408.pdf].
IEA. CoalPower5 database. UK, London: Clean Coal Centre; 2005.
IEA. Energy statistics of OECD countries and non-OECD countries. 2009 ed. Paris: International Energy Agency; 2009.
IPCC. IPCC guidelines for national greenhouse gas inventories. IPCC; 2006 [http://www.ipcc-nggip.iges.or.jp/public/2006gl/index.html].
Janssens-Maenhout G, Pagliari V, Guizzardi G, Muntean M. Global emission inventories in the Emission Database for Global Atmospheric Research (EDGAR) — manual (I). Gridding: EDGAR emissions distribution on global gridmaps. EUR: Publications Office of the European Union; 2013 [25785].
JSIA. Japan soda industry, association. JSIA; 2011 [info retrieved from http://www.jsia.gr.jp].
Kamdem JS. A nice estimation of Gini index and power Pen's parade. Econ Model 2012;29:1299–304.
Karagas MR, Choi AL, Oken E, Horvat M, Schoeny R, Kamai E, et al. Evidence on the human health effects of low-level methylmercury exposure. Environ Health Perspect 2012;120:799–806.
Kos G, Ryzhkov A, Dastoor A, Narayan J, Steffen A, Ariya PA, et al. Evaluation of discrepancy between measured and modelled oxidized mercury species. Atmos Chem Phys 2013;13:4839–63.
Lan X, Talbot R, Castro M, Perry K, Luke W. Seasonal and diurnal variations of atmospheric mercury across the US determined from AMNet monitoring data. Atmos. Chem. Phys. 2012;12:10569–82.
Lee CW, Srivastava RK. Investigation of selective catalytic reduction impact on mercury speciation under simulated NOx emission control conditions. J Air Waste Manag Assoc 2004;54:1560–6.
Lindberg S, Bullock R, Ebinghaus R, Engstrom D, Feng X, Fitzgerald W, et al. A Synthesis of Progress and Uncertainties in Attributing the Sources of Mercury in Deposition, AMBIO. A Journal of the Human Environment 2007;36:19–33.
Mahaffey KR, Sunderland EM, Chan HM, Choi AL, Grandjean P, Marien K, et al. Balancing the benefits of n-3 polyunsaturated fatty acids and the risks of methylmercury exposure from fish consumption. Nutr Rev 2011;69:493–508.
Mahan S, Saviz J. Cleaning up: taking mercury-free chlorine production to the bank. OCEANA-Protecting the World's Oceans; 2007 [http://na.oceana.org/sites/default/files/o/fileadmin/oceana/uploads/mercury/FINAL_Cleaning_Up.pdf].
Maxson PA. Global mercury production, use and trade. In: Nicola Pirrone KRM, editor. Dynamics of mercury pollution on regional and global scales: atmospheric processes and human exposures around the world; 2005. [http://download.springer.com/static/pdf/853/chp%253A10.1007%252F0-387-24494-8_2.pdf?auth66=1391789020_f73839f3c3cb6ea2ad04deb028abde2a&ext=.pdf].
Mergler D, Anderson HA, Chan LHM, Mahaffey KR, Murray M, Sakamoto M, et al. Methylmercury exposure and health effects in humans: a worldwide concern. Ambio 2007;36:3–11.
MOE/Japan. Japan Ministry of the Environment. http://www.env.go.jp/press/press.php?serial=16473, 2013.
Moya JA, Pardo N, Mercier A. Energy efficiency and CO_2 emissions: prospective scenarios for the cement industry; 2010 [EUR 24592 EN – 2010].
Mukherjee A, Bhattacharya P, Sarkar A, Zevenhoven R. Mercury emissions from industrial sources in India and its effects in the environment. In: Mason R, Pirrone N, editors. Mercury fate and transport in the global atmosphere. US: Springer; 2009. p. 81–112.
Müller D, Wip D, Warneke T, Holmes CD, Dastoor A, Notholt J. Sources of atmospheric mercury in the tropics: continuous observations at a coastal site in Suriname. Atmos Chem Phys 2012;12:7391–7.
Munthe J, Wängberg I, Pirrone N, Iverfeldt Å, Ferrara R, Ebinghaus R, et al. Intercomparison of methods for sampling and analysis of atmospheric mercury species. Atmos Environ 2001;35:3007–17.
NADP/AMNet. Atmospheric mercury network. National Atmospheric Deposition Program; 2012 [http://nadp.sws.uiuc.edu/amn/].
NADP/MDN. Mercury deposition network. National Atmospheric Deposition Program; 2012 [http://nadp.sws.uiuc.edu/mdn/].
Olivier J, Janssens-Maenhout G. CO_2 emissions from fuel combustion. IEA CO2 report 2012. Part III, Greenhouse-Gas Emissions, 2012 ed.IEA; 2012.
Pacyna EG, Pacyna JM, Steenhuisen F, Wilson S. Global anthropogenic mercury emission inventory for 2000. Atmos Environ 2006;40:4048–63.
Pacyna EG, Pacyna JM, Sundseth K, Munthe J, Kindbom K, Wilson S, et al. Global emission of mercury to the atmosphere from anthropogenic sources in 2005 and projections to 2020. Atmos Environ 2010;44:2487–99.
Park KS, Seo YC, Lee SJ, Lee JH. Emission and speciation of mercury from various combustion sources. Powder Technol 2008;180:151–6.
Pirrone N, Cinnirella S, Feng X, Finkelman RB, Friedli HR, Leaner J, et al. Global mercury emissions to the atmosphere from anthropogenic and natural sources. Atmos Chem Phys 2010;10:5951–64.
Pirrone N, Aas W, Cinnirella S, Ebinghaus R, Hedgecock IM, Pacyna J, et al. Toward the next generation of air quality monitoring: mercury. Atmos Environ 2013;80:599–611.
Platts. UDI World Electric Power Plants database (WEPP). Platts, McGraw-Hill Companies, Inc.; 2006 [http://www.platts.com/products/world-electric-power-plants-database].
Pudasainee D, Lee SJ, Lee S-H, Kim J-H, Jang H-N, Cho S-J, et al. Effect of selective catalytic reactor on oxidation and enhanced removal of mercury in coal-fired power plants. Fuel 2010;89:804–9.
Pudasainee D, Kim J-H, Yoon Y-S, Seo Y-C. Oxidation, reemission and mass distribution of mercury in bituminous coal-fired power plants with SCR, CS-ESP and wet FGD. Fuel 2012;93:312–8.
Rafaj P, Bertok I, Cofala J, Schöpp W. Scenarios of global mercury emissions from anthropogenic sources. Atmos Environ 2013;79:472–9.
Prestbo EM, Gay DA. Wet deposition of mercury in the U.S. and Canada, 1996–2005: Results and analysis of the NADP mercury deposition network (MDN). Atmos Environ 2009;43:4223–33.
Ryaboshapko A, Bullock Jr OR, Christensen J, Cohen M, Dastoor A, Ilyin I, et al. Intercomparison study of atmospheric mercury models: 2. Modelling results vs. long-term observations and comparison of country deposition budgets. Sci Total Environ 2007;377:319–33.
Selin NE. Global biogeochemical cycling of mercury: a review. Annu Rev Environ Resour 2009;34:43–63.
Selin NE, Jacob DJ, Park RJ, Yantosca RM, Strode S, Jaeglé L, et al. Chemical cycling and deposition of atmospheric mercury: global constraints from observations. J Geophys Res Atmos 2007;112:D02308.
Selin NE, Jacob DJ, Yantosca RM, Strode S, Jaeglé L, Sunderland EM. Global 3-D land–ocean–atmosphere model for mercury: present-day versus preindustrial cycles and anthropogenic enrichment factors for deposition. Global Biogeochem Cycles 2008;22:GB2011.
Slemr F. Worldwide trend of atmospheric mercury since 1977. Geophys Res Lett 2003:30.
Slemr F, Brunke EG, Ebinghaus R, Kuss J. Worldwide trend of atmospheric mercury since 1995. Atmos Chem Phys 2011;11:4779–87.
Soerensen AL, Sunderland EM, Holmes CD, Jacob DJ, Yantosca RM, Skov H, et al. An improved global model for air–sea exchange of mercury: high concentrations over the North Atlantic. Environ Sci Technol 2010;44:8574–80.
Soerensen AL, Jacob DJ, Streets DG, Witt MLI, Ebinghaus R, Mason RP, et al. Multi-decadal decline of mercury in the North Atlantic atmosphere explained by changing subsurface seawater concentrations. Geophys Res Lett 2012;39:L21810.
Srivastava RK, Staudt J, Tavoulareas ES, Jozewicz W, Doorn M. Current and emerging mercury and multipollutant control technologies. ICAC Forum'03: Multi-Pollutant Emission Controls & Strategies, Nashville, TN; 2003. [http://www.icac.com/files/public/ICAC03_Srivastava.pdf].
Steffen A, Douglas T, Amyot M, Ariya P, Aspmo K, Berg T, et al. A synthesis of atmospheric mercury depletion event chemistry in the atmosphere and snow. Atmos Chem Phys 2008;8:1445–82.
Streets DG, Devane MK, Lu Z, Bond TC, Sunderland EM, Jacob DJ. All-time releases of mercury to the atmosphere from human activities. Environ Sci Technol 2011;45:10485–91.
Strode SA, Jaeglé L, Selin NE, Jacob DJ, Park RJ, Yantosca RM, et al. Air–sea exchange in the global mercury cycle. Global Biogeochem Cycles 2007;21:GB1017.
Subir M, Ariya PA, Dastoor AP. A review of uncertainties in atmospheric modeling of mercury chemistry I. Uncertainties in existing kinetic parameters — fundamental limitations and the importance of heterogeneous chemistry. Atmos Environ 2011;45:5664–76.
Subir M, Ariya PA, Dastoor AP. A review of the sources of uncertainties in atmospheric mercury modeling II. Mercury surface and heterogeneous chemistry — a missing link. Atmos Environ 2012;46:1–10.
Swartzendruber PC, Chand D, Jaffe DA, Smith J, Reidmiller D, Gratz L, et al. INTEX-B campaign 2006. J Geophys Res Atmos 2008:113.
Sznopek JL, Goonan T. The material flow of mercury in the economies of the United States and the world. U.S. Geographical Survey Circular, 1197. ; 2000. [http://pubs.usgs.gov/circ/2000/c1197/c1197.pdf].
Takahashi F, Kida A, Shimaoka T. Statistical estimate of mercury removal efficiencies for air pollution control devices of municipal solid waste incinerators. Sci Total Environ 2010;408:5472–7.
Tang S, Feng X, Qiu J, Yin G, Yang Z. Mercury speciation and emissions from coal combustion in Guiyang, southwest China. Environ Res 2007;105:175–82.
Temme C, Einax JW, Ebinghaus R, Schroeder WH. Measurements of Atmospheric Mercury Species at a Coastal Site in the Antarctic and over the South Atlantic Ocean during Polar Summer. Environ Sci Technol 2002;37:22–31.
Telmer K, Veiga M. World emissions of mercury from artisanal and small scale gold mining. In: Pirrone N, Mason R, editors. Interim Report of the UNEP Global Partnership on Atmospheric Mercury Transport and Fate Research. UNEP; 2008. [http://www.mercurywatch.org/userfiles/file/Telmer%20and%20Veiga%202009%20Springer.pdf].
Travnikov O, Ilyin I. The EMEP/MSC-E mercury modeling system. In: Mason R, Pirrone N, editors. Mercury Fate and Transport in the Global Atmosphere. Springer; 2009. p. 571–87.

[http://download.springer.com/static/pdf/515/chp%253A10.1007%252F978-0-387-93958-2_20.pdf?auth66=1392303122_2f556ef607978e1a9cecfce863c61a24&ext=.pdf].

UN. Industrial Commodity Production Statistics Database. United Nations Statistics Division. [info retrieved from http://unstats.un.org/unsd/industry/ics_intro.asp], 2011.

UNEP. Summary of supply, trade and demand information on mercury. UNEP; 2006 [http://www.chem.unep.ch/mercury/PM-HgSupplyTradeDemand-Final-Nov2006-PMformat19Jan07.pdf].

UNEP. Study on mercury sources and emissions, and analysis of cost and effectiveness of control measures "UNEP Paragraph 29 study". Geneva, Switzerland: Division of Technology, Industry and Economics, Chemical Branch; 2010 [http://www.unep.org/hazardoussubstances/Portals/9/Mercury/Documents/Paragraph29Study/Final%20Report%20Para29_5%20Nov%202010.pdf].

UNEP. A practical guide: reducing mercury use in artisanal and small-scale mining. UNEP; 2012 [http://www.unep.org/hazardoussubstances/Portals/9/Mercury/Documents/ASGM/Techdoc/UNEP%20Tech%20Doc%20APRIL%202012_120608b_web.pdf].

UNEP. Global mercury assessment 2013: sources, emissions, releases and environmental transport. Geneva, Switzerland: UNEP Chemicals Branch; 2013a.

UNEP. Minamata convention on mercury. UNEP; 2013b [http://www.mercuryconvention.org/Convention/tabid/3426/Default.aspx].

US_EPA/AP42. Compilation of Air Pollutant Emission Factors. US EPA. [info retrieved from http://www.epa.gov/ttnchie1/ap42/], 2011.

USGS. Mineral operation. U.S. Geological Survey; 2010 [info retrieved from http://tin.er.usgs.gov/mineral-operations/].

USGS. Metal prices in the United States through 2010: U.S. Geological survey scientific investigations report 2012-5188. U.S. Geological Survey; 2013 [http://pubs.usgs.gov/sir/2012/5188].

USGS. Commodity Statistics and Information. U.S. Geographical Survey, [info retrieved from http://minerals.usgs.gov/minerals/pubs/commodity/], 2011.

Wang SX, Zhang L, Li GH, Wu Y, Hao JM, Pirrone N, et al. Mercury emission and speciation of coal-fired power plants in China. Atmos Chem Phys 2010;10:1183–92.

WB. World bank. [info retrieved from http://databank.worldbank.org/data/home.aspx], 2013.

WBCSD. Cement industry energy and CO_2 performance: getting the numbers right. World Business Council for Sustainable Development (WBCSD), The Cement Sustainability Initiative (CSI); 2009 [info retrieved from http://www.wbcsd.org/Pages/EDocument/EDocumentDetails.aspx?ID=11095&NoSearchContextKey].

Won JH, Lee TG. Estimation of total annual mercury emissions from cement manufacturing facilities in Korea. Atmos Environ 2012;62:265–71.

Wu J, Zhang Y, Pan W, He P, Ren J, Shen M, et al. Experimental research on mercury emissions and its speciation in the flue gas from coal-fired power station. International Conference in Energy and Environment Technology; 2009. [http://ieeexplore.ieee.org/stamp/stamp.jsp?tp=&arnumber=5366145].

Wu QR, Wang SX, Zhang L, Song JX, Yang H, Meng Y. Update of mercury emissions from China's primary zinc, lead and copper smelters, 2000–2010. Atmos Chem Phys 2012;12:11153–63.

Zhang L, Blanchard P, Johnson D, Dastoor A, Ryzhkov A, Lin CJ, et al. Assessment of modeled mercury dry deposition over the Great Lakes region. Environ Pollut 2012a;161:272–83.

Zhang Y, Jaeglé L, van Donkelaar A, Martin RV, Holmes CD, Amos HM, et al. Nested-grid simulation of mercury over North America. Atmos Chem Phys 2012b;12:6095–111.

MIT Joint Program on the Science and Policy of Global Change - REPRINT SERIES

FOR THE COMPLETE LIST OF REPRINT TITLES: http://globalchange.mit.edu/research/publications/reprints

2013-33 A Contemporary Carbon Balance for the Northeast Region of the United States, Lu X., D.W. Kicklighter, J.M. Melillo, P. Yang, B. Rosenzweig, C.J. Vörösmarty, B. Gross and R.J. Stewart, *Environmental Science & Technology,* 47(3): 13230–13238 (2013)

2013-34 European-Led Climate Policy versus Global Mitigation Action: Implications on Trade, Technology, and Energy, De Cian, E., I. Keppo, J. Bollen, S. Carrara, H. Förster, M. Hübler, A. Kanudia, S. Paltsev, R.D. Sands and K. Schumacher, *Climate Change Economics,* 4(Suppl. 1): 1340002 (2013)

2013-35 Beyond 2020—Strategies and Costs for Transforming the European Energy System, Knopf, B., Y.-H.H. Chen, E. De Cian, H. Förster, A. Kanudia, I. Karkatsouli, I. Keppo, T. Koljonen, K. Schumacher and D.P. van Vuuren, *Climate Change Economics,* 4(Suppl. 1): 1340001 (2013)

2013-36 Estimating regional methane surface fluxes: the relative importance of surface and GOSAT mole fraction measurements, Fraser, B., P.I. Palmer, L. Feng, H. Boesch, A. Cogan, R. Parker, E.J. Dlugokencky, P.J. Fraser, P.B. Krummel, R.L. Langenfelds, S. O'Doherty, R.G. Prinn, L.P. Steele, M. van der Schoot and R.F. Weiss, *Atmospheric Chemistry and Physics,* 13: 5697–5713 (2013)

2013-37 The variability of methane, nitrous oxide and sulfur hexaflouride in Northeast India, Ganesan, A.L., A. Chatterjee, R.G. Prinn, C.M. Harth, P.K. Salameh, A.J. Manning, B.D. Hall, J. Mühle, L.K. Meredith, R.F. Weiss, S. O'Doherty and D. Young, *Atmospheric Chemistry and Physics,* 13: 10633–10644 (2013)

2013-38 Integrated economic and climate projections for impact assessment, Paltsev, S., E. Monier, J. Scott, A. Sokolov and J.M. Reilly, *Climatic Change*, October 2013, doi: 10.1007/s10584-013-0892-3 (2013)

2013-39 Fiscal consolidation and climate policy: An overlapping generations perspective, Rausch, S., *Energy Economics,* 40(Supplement 1): S134–S148 (2013)

2014-1 Estimating a global black carbon emissions using a top-down Kalman Filter approach, Cohen, J.B. and C. Wang, *Journal of Geophysical Research—Atmospheres,* 119: 1–17, doi: 10.1002/2013JD019912 (2014)

2014-2 Air quality resolution for health impact assessment: influence of regional characteristics, Thompson, T.M., R.K. Saari and N.E. Selin, *Atmospheric Chemistry and Physics,* 14: 969–978, doi: 10.5194/acp-14-969-2014 (2014)

2014-3 Climate change impacts on extreme events in the United States: an uncertainty analysis, Monier, E. and X. Gao, *Climatic Change,* doi: 10.1007/s10584-013-1048-1 (2014)

2014-4 Will economic restructuring in China reduce trade-embodied CO_2 emissions? Qi, T., N. Winchester, V.J. Karplus, X. Zhang, *Energy Economics,* 42(March): 204–212 (2014)

2014-5 Assessing the Influence of Secondary Organic versus Primary Carbonaceous Aerosols on Long-Range Atmospheric Polycyclic Aromatic Hydrocarbon Transport, Friedman, C.L., J.R. Pierce and N.E. Selin, *Environmental Science and Technology,* 48(6): 3293–3302 (2014)

2014-6 Development of a Spectroscopic Technique for Continuous Online Monitoring of Oxygen and Site-Specific Nitrogen Isotopic Composition of Atmospheric Nitrous Oxide, Harris, E., D.D. Nelson, W. Olszewski, M. Zahniser, K.E. Potter, B.J. McManus, A. Whitehill, R.G. Prinn and S. Ono, *Analytical Chemistry,* 86(3): 1726–1734 (2014)

2014-7 Potential Influence of Climate-Induced Vegetation Shifts on Future Land Use and Associated Land Carbon Fluxes in Northern Eurasia, Kicklighter, D.W., Y. Cai, Q. Zhuang, E.I. Parfenova, S. Paltsev, A.P. Sokolov, J.M. Melillo, J.M. Reilly, N.M. Tchebakova and X. Lu, *Environmental Research Letters,* 9(3): 035004 (2014)

2014-8 Implications of high renewable electricity penetration in the U.S. for water use, greenhouse gas emissions, land-use, and materials supply, Arent, D., J. Pless, T. Mai, R. Wiser, M. Hand, S. Baldwin, G. Heath, J. Macknick, M. Bazilian, A. Schlosser and P. Denholm, *Applied Energy,* 123(June): 368–377 (2014)

2014-9 The energy and CO_2 emissions impact of renewable energy development in China, Qi, T., X. Zhang and V.J. Karplus, *Energy Policy*, 68(May): 60–69 (2014)

2014-10 A framework for modeling uncertainty in regional climate change, Monier, E., X. Gao, J.R. Scott, A.P. Sokolov and C.A. Schlosser, *Climatic Change,* online first (2014)

2014-11 Markets versus Regulation: The Efficiency and Distributional Impacts of U.S. Climate Policy Proposals, Rausch, S. and V.J. Karplus, *Energy Journal*, 35(SI1): 199–227 (2014)

2014-12 How important is diversity for capturing environmental-change responses in ecosystem models? Prowe, A. E. F., M. Pahlow, S. Dutkiewicz and A. Oschlies, *Biogeosciences*, 11: 3397–3407 (2014)

2014-13 Water Consumption Footprint and Land Requirements of Large-Scale Alternative Diesel and Jet Fuel Production, Staples, M.D., H. Olcay, R. Malina, P. Trivedi, M.N. Pearlson, K. Strzepek, S.V. Paltsev, C. Wollersheim and S.R.H. Barrett, *Environmental Science & Technology*, 47: 12557–12565 (2013)

2014-14 The Potential Wind Power Resource in Australia: A New Perspective, Hallgren, W., U.B. Gunturu and A. Schlosser, *PLoS ONE,* 9(7): e99608, doi: 10.1371/journal.pone.0099608 (2014)

2014-15 Trend analysis from 1970 to 2008 and model evaluation of EDGARv4 global gridded anthropogenic mercury emissions, Muntean, M., G. Janssens-Maenhout, S. Song, N.E. Selin, J.G.J. Olivier, D. Guizzardi, R. Maas and F. Dentener, *Science of the Total Environment,* 494-495(2014): 337-350 (2014)

For limited quantities, Joint Program Reprints are available free of charge. Contact the Joint Program Office to order.